

Hybrid Rendering for Dynamic Scenes

Alexandr Kuznetsov
alexandr.kuznetsov@intel.com
Intel Corporation
USA

Anton Sochenov
anton.sochenov@intel.com
Intel Corporation
USA

Stavros Diolatzis
stavros.diolatzis@intel.com
Intel Corporation
France

Anton Kaplanyan
anton.kaplanyan@intel.com
Intel Corporation
USA



Figure 1. Inserting arbitrary dynamic objects into static scenes. Our method can render it efficiently by taking a static scene and then adding the light transport difference: $L_{\Delta} = L_{+} - L_{-}$. By using a pretrained network to represent the light transport in the static scene, we can quickly "render" it without path-tracing and any noise. The difference light transport, L_{Δ} has much less noise than rendering from scratch.

Abstract

Despite significant advances in algorithms and hardware, global illumination continues to be a challenge in the real-time domain. Time constraints often force developers to either compromise on the quality of global illumination or disregard it altogether. We take advantage of a common setup in modern games: having a set of a level, which is a static scene with dynamic characters and lighting. We introduce a novel method for efficiently and accurately rendering global illumination in dynamic scenes. Our hybrid technique leverages precomputation and neural networks to capture the light transport of a static scene. Then, we introduce a method to compute the difference between the current scene and the static scene, which we already precomputed. By

handling the bulk of the light transport through precomputation, our method only requires the rendering of a minimal difference, reducing the noise and increasing the quality.

Keywords: Neural Rendering, Path-Tracing, Hybrid Rendering, Global Illumination

1 Introduction

Rendering photo-realistic images is a fundamental problem in computer graphics. With advances in hardware, physically accurate path tracing became possible. This allows physically accurate light simulations. However, full path tracing is an expensive endeavor, especially in real-time applications such as games. With the current hardware, even in simple scenes, the amount of rays per pixel is quite limited. As a result, heavy denoising needs to be applied which significantly blurs and degrades the quality of an image. An alternative

option is to precompute global illumination via deep learning for example. This works extremely well in static scenes. However, it fails when anything changes in the scene. This is because of the curse of dimensionality. Instead of learning a 4D function (2 for space and 2 for directions) for a static scene, for a dynamic scene, you need to learn a 7D+ function, requiring enormous datasets and long training. Besides, such systems cannot display novel objects, which severely limits their use cases. Therefore, pure precomputation for dynamic scenes is not practical. In this paper, we combine the benefits of using precomputations for a static portion of a scene and using path tracing for the dynamic portion of the light transport.

One of the major applications of our method is games. Real-time global illumination is challenging and it slowly becoming a reality due to advances in hardware raytracing. Games are usually made of levels, which are mostly static with movable objects and characters. In those applications, a scene is rendered in every frame. However, the light transport in the scene doesn't change much from frame to frame. We want to take advantage of this property in order to accelerate the rendering of global illumination. To do that, we separate the scene into static and dynamic parts. Assuming we can render the static parts of the scene quickly with the help of a precomputation, the task is to render the changes caused by the dynamic part of the scene. In this paper, we will look at how we can render changes in the light transport caused by dynamic objects and lights.

The goal of the paper is to introduce the idea of the hybrid rendering. The faster rendering more realistic computer graphics in real-time domains such as games. The key contributions of our paper are as follows:

- We introduce the idea of hybrid rendering of static scenes with *arbitrary* dynamic objects and dynamic lights. By separating a scene into precomputed static and sparse dynamic light transport, we can more efficiently render both.
- Our method supports the addition of arbitrary dynamic objects.
- We introduce a mathematical justification and show that the method is conditionally unbiased.
- We also make the connection to the Primary Space Sampling.

Our method combines the benefits of precomputation and adaptive path-tracing, to render efficiently render global illumination in real-time.

2 Related Work

In this section, we review related work from path tracing, precomputation techniques, neural rendering & denoising and finally adaptive approaches. Each one of these fields is active and vast so we review methods closest to our approach,

while referring to surveys whenever possible for an extensive overview.

2.1 Path Tracing

Monte Carlo estimators in the context of path tracing have been used extensively to create realistic-looking images of synthetic scenes and a lot of research has gone into improving their sampling quality to generate these images faster. These images are plagued with noise, inherent in Monte Carlo estimators and different variance reduction techniques, such as importance sampling, control variates and sample reuse have been proposed to get cleaner images with less samples.

In the past the evaluation of visibility between two surfaces was too costly for interactive applications leading to innovative work like [Dachsbacher et al. 2007] which avoided this computation by implicitly defining visibility through antiradiance. Our method is inspired by this concept but we aim to use our formulation only for the parts of a scene that have changed given a precomputed image/radiance field.

The emergence of path tracing hardware [Keller et al. 2015] opened the door to real-time path tracing, a long-standing goal of computer graphics. Despite the recent advances in hardware, the sampling budget in interactive applications is still restricted to a few samples per pixel, compared to the hundreds or thousands used in offline rendering. With this restriction in mind, ReSTIR and variants [Bitterli et al. 2020; Lin et al. 2022; Ouyang et al. 2021] propose to reuse samples either temporally or spatially, increasing the effective sample count in cases of coherent content between frames and pixels. Reuse is less useful for hard-to-sample effects, such as caustics and specular-diffuse-specular paths, which need hundreds of samples to even appear and as a result, they are either treated explicitly or avoided. Our method is orthogonal to ReSTIR and can be easily integrated to work together with ReSTIR.

2.2 Precomputation Techniques

Related to our method, there is a long history of precomputation techniques that use information from a one-time preprocessing step to improve the quality of rendering during runtime. Ward et al. [Ward et al. 1988] precomputes the outgoing radiance within a scene and stores it explicitly in a spatial cache. During rendering an interpolation scheme is used, ignoring view dependency, to infer the outgoing radiance at any point in the scene. This was improved upon by [Krivánek et al. 2005] to take into account the viewing direction encoded by spherical harmonics while illumination gradients improved the interpolation. In [Zhou et al. 2005] the authors suggest the precomputation of shadow fields and use them to efficiently compute soft shadows for dynamic scenes. Precomputation using low rank operators and proxy shapes was introduced in [Loos et al. 2011] and improved upon in [Loos et al. 2012] which has the advantage of being

a scene-independent precomputation technique but suffers in terms of quality compared to the ground truth.

More recently, many pre-baking systems [Seyb et al. 2020; Silvennoinen and Sloan 2021] have been developed using multiple components and data structures that have been engineered to enable dynamic changes to some aspects of the precomputed radiance transfer. Our methods explore how real-time path tracing can augment images of static components in a scene with dynamic content. The static component can also be precomputed as in this previous work.

2.3 Neural Rendering & Denoising

Neural networks have been used to render images in the context of synthetic scenes, novel view synthesis and generative models in the rapidly growing field of neural rendering. An overview of the field can be found in [Tewari et al. 2022]. We focus on the use of neural networks to replace, augment or speed up rendering of synthetic scenes.

A first attempt at using neural networks to regress the radiance of a given scene was proposed in [Ren et al. 2013]. Here a Multi-Layer Perceptron (MLP) is trained to infer the outgoing radiance for any point in the scene given the world position, viewing direction, BSDF parameters etc. In a similar spirit, the work by Granskog et al. [Granskog et al. 2020] renders a scene from different viewpoints and uses them to create a compositional neural scene representation to shade easy-to-compute G-Buffers. An object-oriented approach proposed by [Zheng et al. 2023] composed a scene by combining neural networks that represent each object’s impact in light transport.

Operating in image space [Nalbach et al. 2017] uses a convolutional neural network (CNN) within a deferred shading step to speed up the rendering of effects such as ambient occlusion, depth of field, etc. CNNs have also been shown to be efficient denoisers leading to clean images with much less samples. [Bako et al. 2017] uses two deep networks, one for the diffuse and one for the specular component, which take G-buffers as input and are trained to reduce the noise of an input image. Gharbi et al. [Gharbi et al. 2019] use a denoising network that operates on the input samples of the rendering, instead of the collapsed image. This leads to better performance since the network has more information about the underlying effects of the image. [Işık et al. 2021] proposes the use of a lightweight network to enable denoising at interactive rates while being temporally stable. Denoising can also be combined with supersampling [Thomas et al. 2022] enabling rendering in lower sample counts *and* resolution. The path-tracing component of our method can benefit from a denoising/supersampling step to improve the quality of the final image.

MLPs which operate in world space, similar to [Ren et al. 2013], have recently gained popularity due to their inherent view consistency and ability to implicitly represent the radiance fields of a given scene from sparse training data.

In [Müller et al. 2021] a small network is used as a radiance cache which is constantly trained and updated on the fly. This cache is used to guide paths and terminate them early. This approach enables the use of a predicting neural network in a fully dynamic scene but comes with the trade-off of allocating a compute bandwidth to constantly train and update the network. To pretrain an MLP and learn the radiance field for a variable scene, [Diolatzis et al. 2022] encode the predetermined variability of a scene into a conditioning vector. While this shows promising quality for traditionally hard-to-render effects the variability is limited to a few predetermined factors. We aim to alleviate this issue of pretrained neural radiance fields by efficiently combining their outputs with path tracing.

2.4 Adaptive Methods

Our method is most closely related to adaptive methods, which guide sample placement during path tracing to reduce the noise in the final image. We specifically focus on adaptive methods that combine path tracing with a neural component and refer to [Zwicker et al. 2015] for an overview of more traditional approaches.

In [Kuznetsov et al. 2018] the authors propose a denoising-aware sample placement approach. Two CNNs are trained end to end, one learns to create a sampling map which is used to render the noisy image, and another denoises that image. This leads to increased sample placement in areas where the denoiser needs more information. This also has been shown to work effectively in the temporal domain [Hasselgren et al. 2020] by using information from temporally reprojected previous frames. Recently analytic distributions [Salehi et al. 2022] have been proposed to guide the sample placement before a denoising step from denoising performance. Our approach draws inspiration from the adaptive nature of these methods but focuses on the scenario of augmenting a pre-computed image/representation with new dynamic content. Parallels can also be drawn between our method and [Rouselle et al. 2016] which formulates the problem as image-based control variates. They use a pre-rendered image with a computed difference given changed materials. However, their method requires a fixed camera, making it impractical in real-world applications. Our method utilizes the recent advances in neural networks to enable a moving camera and adds support for dynamic objects and lights, which opens up a whole new realm of possibilities. Our adaptive sampling exploits the sparsity of the delta light transport to improve the quality even further.

3 Method

Our method has two major components: rendering dynamic light transport and rendering static light transport. The basic idea of our method is we can quickly render the light transport of the static scene and then adaptively render the light

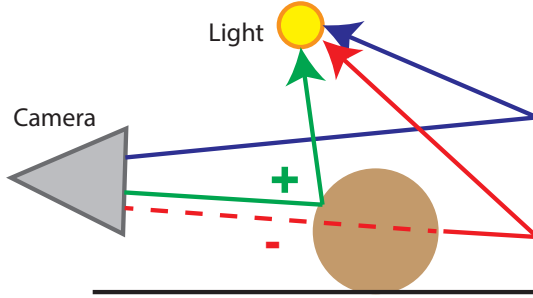


Figure 2. Example of different paths during rendering a scene. Here, we have a beige sphere as a dynamic object. The blue path $\in \Omega_0$ doesn't interact with the dynamic object. The green path $\in \Omega_+$ reflects from the dynamic object. And the red path $\in \Omega_-$ goes directly through the dynamic object unaffected.

transport caused by dynamic objects. First, we will look into how we can incorporate the rendering of dynamic objects. Then we will take a look at how we can render static scenes.

3.1 Rendering Dynamic Light transport

In order to render a scene with dynamic objects, we want to render the static scene, plus the light transport delta caused by adding the dynamic objects to the scene:

$$\begin{aligned} L_H &= L_s + (L_+ - L_-) \\ L_H &= L_s + L_\Delta \end{aligned} \quad (1)$$

where L_H is the light transport of the scene with the dynamic objects, L_s is the light transport of the static scene (without the dynamic objects), L_+ is the additive light transport caused by adding the dynamic objects, and L_- is the subtractive light transport caused by adding the dynamic objects. See Figure 2 for details. Computing L_s can be achieved through classical path-tracing or through precomputation as will be discussed in the next section. The crux is how can we compute L_+ and L_- .

Additive Light Transport. Here, we will discuss how we compute L_+ . This is an additional radiance contribution caused by adding the dynamic objects. For example, by adding a green sphere, we will get green inter-reflection on the floor. We can define it as the light contribution caused by adding the dynamic objects. So, we start accumulating the radiance only after the path is reflected by a dynamic object. Please refer to Algorithm 1 for the implementation details. The algorithm can easily be extended to support Multiple Importance Sampling.

Subtractive Light Transport. Here, we will discuss how we compute L_- . This is a subtractive radiance contribution caused by adding dynamic objects. For example, adding a cube in front of the light will cause a shadow that wasn't

Algorithm 1 Calculating L_+

```

1:  $L_+ \leftarrow 0$  ▷ Additive Radiance
2:  $T \leftarrow 1$  ▷ Transmittance
3:  $h \leftarrow \text{false}$  ▷ Did we hit a dynamic object yet?
4:  $r \leftarrow \text{INITIALRAY}()$ 
5: while true do
6:    $\text{bsdf} \leftarrow \text{RAYINTERSECT}(r, S \cup D)$  ▷ Scene with
   Dynamic
7:    $h \leftarrow h \vee \text{IsDYNAMIC}(\text{bsdf})$ 
8:   if  $h$  then
9:      $L_+ \leftarrow L_+ + T \cdot \text{EMMITER}(r, \text{bsdf})$ 
10:  end if
11:   $r, T \leftarrow \text{SAMPLEBSDF}_+(\text{bsdf}, r, T)$ 
12:   $T \leftarrow \text{RUSSIANROULETTE}(T)$ 
13:  if  $T=0$  then
14:    break
15:  end if
16: end while
17: return  $L_+$ 

```

Algorithm 2 Calculating L_-

```

1:  $L_- \leftarrow 0$  ▷ Subtractive Radiance
2:  $T \leftarrow 1$  ▷ Transmittance
3:  $h \leftarrow \text{false}$  ▷ Did we hit a dynamic object yet?
4:  $r \leftarrow \text{INITIALRAY}()$ 
5: while true do
6:    $\text{bsdf} \leftarrow \text{RAYINTERSECT}(r, S \cup D)$  ▷ Scene with
   Dynamic
7:    $d \leftarrow \text{IsDYNAMIC}(\text{bsdf})$ 
8:    $h \leftarrow h \vee d$ 
9:   if  $d$  then ▷ Ignore dynamic objects
10:     $r \leftarrow \text{SKIPOBJECT}(r)$ 
11:    continue
12:  end if
13:  if  $h$  then
14:     $L_- \leftarrow L_- + T \cdot \text{EMMITER}_-(r, \text{bsdf})$  ▷ Accum.
   radiance
15:  end if
16:   $r, T \leftarrow \text{SAMPLEBSDF}(\text{bsdf}, r, T)$ 
17:   $T \leftarrow \text{RUSSIANROULETTE}(T)$ 
18:  if  $T=0$  then
19:    break
20:  end if
21: end while
22: return  $L_-$ 

```

present in the static scene. The subtractive contribution or L_- is just the accumulation of all the light paths in the static rendering, which would go through the dynamic objects if they were present. So, in order to calculate L_- , we just need to re-render the static scene and accumulate only the contributions after the ray goes through a dynamic object.

Here, we treat the dynamic objects as totally transparent. Please, refer to the Algorithm 2 to see how to compute L_- . Similarly, this algorithm is trivially extended to MIS.

3.2 Mathematical Justification

Here we will prove that our definitions the Equation 1 hold true with the given definitions. Classically, the rendering equation is written like this:

$$L(x, \omega_o) = L_e(x, \omega_o) + \int f(x, \omega_i, \omega_o) \cdot G(x, x') d\omega_i \quad (2)$$

where L_e is the emission radiance on the surface, $f()$ is the cosine weighted BSDF term and $G()$ is the geometric visibility term. This equation can be rewritten as an integral over all possible paths in the scene between the camera and all the emitters:

$$L(x, \omega_o) = \int_{\Omega(x, \omega_o)} T(\mathcal{X}) L_e(\text{last}(\mathcal{X})) d\mathcal{X} = I(\Omega(x, \omega_o)) \quad (3)$$

where $\Omega(x, \omega_o)$ is a set of possible paths \mathcal{X} in the scene which start at x and direction ω_o and end at an emitter, and $T()$ is the transmittance of the path. As a shortcut, from now on we will refer to $\Omega(x, \omega_o)$ as simply Ω .

Now let's define the following path domains as a subset of all possible paths in a space: Ω_o - a path that doesn't go through any dynamic object (blue in Fig. 2), Ω_- - a path that ignores dynamic objects (red), and Ω_+ - a path that interacts with every dynamic object it encounters (green). See figure 2 for the illustration. Those are disjoint sets, s.t.:

$$\Omega_o \cup \Omega_- \cup \Omega_+ = \Omega \quad (4)$$

Then, we can rewrite L_s and L_H as follows:

$$\begin{aligned} L_s &= I(\Omega_o) + I(\Omega_-) \\ L_d &= I(\Omega_o) + I(\Omega_+) \end{aligned} \quad (5)$$

By combining the equations we get:

$$\begin{aligned} L_d &= I(\Omega_o) + (I(\Omega_-) - I(\Omega_-)) + I(\Omega_+) \\ &= (I(\Omega_o) + I(\Omega_-)) - I(\Omega_-) + I(\Omega_+) \\ &= L_s - I(\Omega_-) + I(\Omega_+) \\ &= L_s - L_- + L_+ = L_s + L_\Delta \end{aligned} \quad (6)$$

As a result, we can see that our method is unbiased as every integrator is unbiased. Later, we will replace the static scene renderer $I(\Omega_o)$, with a neural network, which is biased.

3.3 Primary Sample Space

Primary Sample Space is the idea of operating on a hypercube of random numbers. It was first popularized by Kelemen et al. [Kelemen et al. 2002] to simplify the Metropolis Light Transport algorithm. We found utilizing primary sample space also simplifies the integration of our algorithm into existing engines. We used this method, to integrate our method with the real-time path tracer Falcor. Later, we will show

that those two approaches are equivalent. PSS duplicates the computation of the paths that haven't diverged. However, we didn't find a severe negative impact on performance.

The algorithm is described in 3. Instead of tracing the ray until we hit a dynamic object and splitting the ray into two, we render the same scene twice. First, we render the static scene and then we render the dynamic scene. If we do that naively, the noise will be not correlated and we get the different image which is noisy. However, if we use primary sample space and reuse the random numbers for the both renders, the noise pattern will be correlated. This is because it will diverge only if the ray hits a dynamic object. As a result, the different images will have much less noise compared to individual renderings.

Using primary sample space algorithm 3 is equivalent to calculating the difference we get from 1 and 2 algorithms. This is because until we hit a dynamic object, we trace the same paths. If we use the same random numbers in 1 and 2, the path will be exactly the same. Therefore, it will produce the same result.

3.4 Static Scene Rendering

Although we can render simply L_s , this will defeat the purpose of the method as rendering L_H is not much more expensive. Therefore, we want to precompute the light transport for the static scene. Because the scene is static, this is a relatively simple thing to do. We need to learn just a 5D function $\tilde{L}_s(x, \omega)$ - 3 dimensions for the position of the ray and 2 for direction. This task can be approached in a number of ways, but we chose to utilize a hash grid with an MLP. Inspired by [Müller et al. 2021], given a 3D location of the intersection, we look up a corresponding latent vector in the hierarchical hash grid. Then, we concatenate the latent vector with camera direction and surface normal vectors and pass it to the MLP. The MLP consists of 7 hidden layers with 64 channels in each. It outputs the final radiance information. As the network is small and operates in screen space (unlike volumetric NeRF-like methods), the runtime is negligible.

In order to train the network, we first must generate a dataset of the static scene. This is done by originating the rays at random inside the scene going to random directions. We used 1×10^9 ray samples to train our network. Unlike [Müller et al. 2021], we pretrain the network offline for 2 hours and only do inference during the runtime. That way, we don't need to do ray-tracing and training during the runtime, saving us the compute at the expense of bias.

3.5 Adaptive Sampling

Adaptive Sampling is a crucial part of our method. L_Δ , the difference in light transport is very sparse. The majority of the difference is located near a dynamic object or a dynamic light. Therefore, we can use adaptive sampling to focus on

those regions. Because those regions are typically small compared to the overall image size, we can spend much more samples in those regions. Because in the rest of the image, L_Δ is close to zero, allocating fewer samples there doesn't contribute to a higher error.

There are different strategies for adaptive sampling. One way is to make an initial pass at a lower resolution or sampling count in order to estimate the sampling map as it was done in [Kuznetsov et al. 2018]. The other way is to exploit the temporal information from the previous frames to estimate the sampling map for the current frame as was done in [Hasselgren et al. 2020]. The advantage of this approach is that there are no extra samples you need to render.

There are different ways to estimate the sampling map from the SURE-based estimator to a neural network. However, we opted for a simpler approach: the samples are distributed proportional to the variance and intensity of the samples. We found this approach is really fast and generates sufficiently good sampling maps.

$$s_i = S \cdot \frac{\sigma(L_{\Delta i}) + |L_{\Delta i}|}{1/N \sum_j \sigma(L_{\Delta j}) + |L_{\Delta j}|} \quad (7)$$

where s is the sample count for the pixel i , S is the target sample count, and N is the total number of pixels in the image. Because the estimates of the variance and intensity are noisy, we apply a simple Gaussian filter with a kernel of size 5, which removes the noise. Then we normalize the sampling map to the desired sampling count and apply a dither operation to discretize the sampling map.:

$$\hat{s}_i = \text{round}(s_i + U) \quad (8)$$

where U is the random value between -0.5 and 0.5

With this direct approach, two problems arise: bias and exploration. Some regions of the image are of very low intensity and variance, so they get a total of 0 samples per pixel across the whole image. This introduces bias because we assume that there are no differences, while there might be. And second of all, because we use previous frames to predict the sampling maps, it creates a positive feedback loop where we don't render anything, so the variance is zero, and so on. To mitigate this issue, we set the minimum number of samples to be 1 per 4 pixels. That way we always have an estimate of variance and intensity anywhere in the image. This solves the sampling map problem, but not the bias. Inspired by Russian Roulette, we propose to divide the intensity by the pre-quantized sampling map.

$$\hat{L}_\Delta = \frac{L_\Delta}{\min(1, s)} \quad (9)$$

That way we compensate for the pixels we didn't render.

See the algorithm 3 for details.

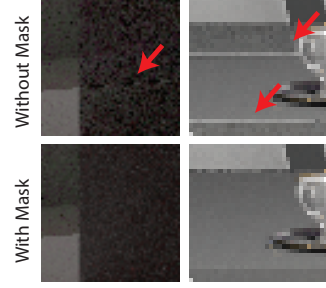


Figure 3. Example of hybrid rendering with and without the mask. Without the mask, we get visible artifacts at the edges due to the difference between the real base image and the learned-based image. The background error is leaking through the dynamic objects. Due to the nature of artifacts, it's hard for a denoiser to get rid of them.

Algorithm 3 Calculating difference using PSS

```

1:  $L_+ \leftarrow 0$                                  $\triangleright$  Radiance of the new scene
2:  $L_- \leftarrow 0$                                  $\triangleright$  Radiance of the static scene
3:  $T_+ \leftarrow 1$                                  $\triangleright$  Transmittance of new
4:  $T_- \leftarrow 1$                                  $\triangleright$  Transmittance of static
5:  $u_0, u_1, u_2 \dots \leftarrow \text{INITRANDOMSEQUENCE}()$   $\triangleright$  List of
   random numbers
6:  $r_+ \leftarrow \text{INITIALRAY}()$ 
7:  $r_- \leftarrow \text{INITIALRAY}()$ 
8: for  $i \leftarrow 0$  to  $\infty$  do
9:    $r_+, T_+ \leftarrow \text{INTERSECTANDSAMPLE}(u_i, \text{bsdf}_+, r_+, T_+)$ 
10:   $r_-, T_- \leftarrow \text{INTERSECTANDSAMPLE}(u_i, \text{bsdf}_-, r_-, T_-)$ 
11:   $L_+ \leftarrow L_+ + T_+ \cdot \text{EMMITER}_+(r_+, \text{bsdf}_+)$ 
12:   $L_- \leftarrow L_- + T_- \cdot \text{EMMITER}_-(r_-, \text{bsdf}_-)$ 
13:   $T_+, T_- \leftarrow \text{RUSSIANROULETTE}(T_+, T_-)$ 
14:  if  $T=0$  then
15:    break
16:  end if
17: end for
18: return  $L_+ - L_-$ 

```

3.6 Dynamic Lights

In games and other scenarios, it's common for the lighting to change. Our method can also support changing illumination. When a light moves, it doesn't affect the whole scene equally. Due to the inverse square law, the moving light affects surfaces closest to the light source the most. For example, if you move a light near a wall, the wall's brightness changes dramatically, but the overall illumination of a room doesn't change. Our algorithm can support dynamic lights combined with dynamic objects. Please, see Fig. 7 for examples. This requires a simple change in the light evaluation function. When evaluating the light contribution for L_+ and L_- , we need to use the corresponding state of the light.

Environment Maps. Often a scene is illuminated by an environment map. Often that environment map changes from frame to frame. For example, clouds move through the sky or the sun moves. It would be a complete waste to start from scratch and completely re-render the scene. Instead, we want to use an existing rendering and modify it to reflect a new environment map. See Fig 5 for the example. To improve the quality further, we employ the standard important sampling. Unlike the traditional environment maps, E_Δ might have negative values. Therefore, when we import sample the environment map, we should sample proportionally to $|E_\Delta|$.

3.7 Masked Rendering

Although the equation 1 is mathematically correct and unbiased, it assumes that L_s is also unbiased. As we have seen from the previous section, this is might not the case. Because of the biases in \tilde{L}_s , the equation 1 is no longer valid. This causes artifacts as shown in Figure 3. To avoid this, we propose to mask out the direct contribution of the dynamic objects. Let \mathbb{M} be the mask that excludes all dynamic objects in the first bounce. Then:

$$\tilde{L}_H \approx \mathbb{M} \times (\tilde{L}_s - L_-) + L_+ \quad (10)$$

From Algorithms 1 and 2, we can see that if we hit the dynamic object first, then $L_H = L_+$ and $L_s = L_-$. So, we can safely ignore the non-zero error $\tilde{L}_s - L_-$ when we hit a dynamic object first

3.8 Denoising and Other Improvements

Our method can be used with a denoiser as seen in Fig. 4. Our method decreases the noise, which improves the quality of denoised images.

Our method is orthogonal to other techniques used to accelerate the rendering. For example, our method can be easily used with path-guiding methods. Instead of using the SampleBSDF function, we substitute it with a sampling function from a path-guiding algorithm. A small modification that’s needed is to use the same path-guiding state across algorithms 1 and 2. That way the sampling function would behave identically. A further improvement can be achieved by training path-guiding on the difference L_Δ instead of overall intensity.

Similarly, it can be combined with ReSTIR [Bitterli et al. 2020]. ReSTIR improves the sampling of lights. Similar to the path-guiding case, we just need the same state across algorithms 1 and 2. That way samples will stay correlated.

4 Results

In this section, we discuss the performance of our method across different scenes in a variety of scenarios. First, we will discuss how our method performs in adding an object to a scene scenario. Then, we will see how our method helps a denoiser generate better images. Then, we will see what will

happen if we also change the lighting. Then, we will see how we can use our method with changing environment maps.

In figure 6 we have a comparison of our method to path tracing. Here, we inserted a completely novel object. It alters the light transport of a scene in a nontrivial way. The left-most images are images using our method. Here, we used a neural network to compute the base image of the static scene and only 1spp on average to compute the difference. Next, we have images of the static scenes. We used the complete light transport of those scenes to train the neural network. In the first column of the comparisons, we have a path-traced image using 2spp. As you can, the results are quite noisy everywhere, which makes it hard to see the details of complex scenes. If we want to use a path-tracer in games, it’s clear that 2spp is not enough. Next, we have our method without adaptive sampling. It uses just 1spp, which is equivalent to 2spp in a path tracer because we need to trace both L_+ and L_- contributions. Here, the images are still noisy where the dynamic objects are (top row), but they are almost noise-free in the areas that aren’t dynamic objects. This is because we used a neural representation for the base image, which is noise-free. So, the noise is only coming from the $L_+ - L_-$ difference. Because those samples are correlated, the error is much lower than from path tracing. The second to last column is our method with adaptive sampling. In the previous column, some regions were noise-free, while others were quite noisy. We can redistribute the samples to the regions where they are needed the most. By doing so, we increase the quality without increasing the sampling budget. Our method resembles the reference images even without a denoiser. Please see the supplemental materials for full-sized images.

We can use a denoiser to improve the result even further. In figure 4 we applied the Optix denoiser. As you can see, the path-traced result is quite blurry. For example, there is not enough information to reconstruct the fireplace in the living room scene or the shadow in the staircase scene. This is because the inputs are quite noisy as we saw in Fig. 6. Our method makes the input images less noisy, which translates to a better reconstruction. Unlike traditional path-tracers, the characteristics of our noise are quite different. It’s a sparse pepper and salt whose value can be actually negative. Despite this, the pretrained denoiser handles our method quite well. But we believe that training a denoiser directly on our method would have improved our results even further,

Not only an object can be changed in a scene. Often the lighting changes as well. In fig. 7 we have the scenes where not only an object was added, but also the lighting has changed. This is a more challenging scenario because L_Δ is no longer that sparse. Nevertheless, our method works pretty well in all the scenes.



Figure 4. Example of our method with a denoiser applied. The 1st column is path-traced images with 2 spp. The 2nd column is our method with just one 1spp. The next to last column is our method with adaptive sampling. Even without the adaptive sampling, our method is much better compared to the path-tracer. Our method lowers the noise level in the input to the denoiser, which improves the quality of the denoiser.

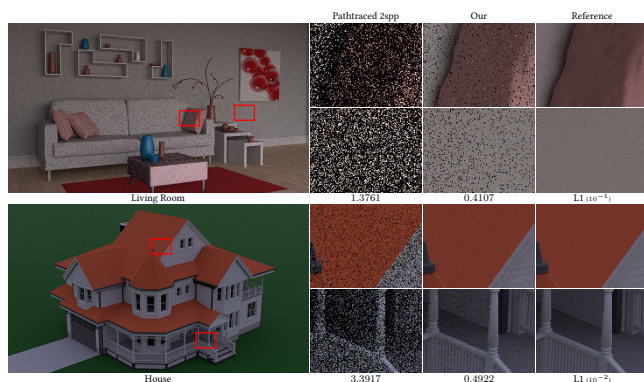


Figure 5. Scenes illuminated by changing environment lighting. In path tracing, we need to render everything from scratch. In our method, we only render the difference, leading to less noise.

In Fig. 5 we show the results with changing environment maps. For the path-tracer, we need to integrate the environment map, which requires a lot of samples. Many contributions here are zero because they are coming from behind. Our method works much better because we sample the difference in the environment maps.

Video comparisons. We also include video comparisons in the supplemental materials. Our method is temporally stable. Moreover, because our method has a lower noise level, the denoiser can handle the input better, creating reference-like results without flickering artifacts. We implemented our method in Falcor and we achieve real-time performance (30-50fps depending on a scene). The FPS depends on scene complexity, but 1 spp of our method is about the same performance as the path-tracer with 2spp because we need to

trace for L_+ and L_- . The static scene evaluation is negligible because it’s done on the auxiliary buffers on tensor cores part of the GPU.

5 Conclusion and Future Work

In conclusion, we presented a novel method for rendering hybrid scenes: a static scene with arbitrary dynamic objects and dynamic lights. We used a neural network to represent the static scene and use then path traced the difference. The samples are correlated, leading to smaller errors and faster convergence time. Our approach is opening new possibilities in the rendering of global illumination in real-time applications like games, where you have mostly static levels with movable characters. As we have shown, L_+ and L_- are really sparse. Therefore we utilize adaptive sampling to smartly allocate samples to reduce the noise. In future works, we would like to explore the importance sampling of dynamic objects in order to reduce the error. Also, we used off-the-shelf denoiser, which worked really well. We would like to design a denoiser that can better handle the negative noise.

References

- Steve Bako, Thijs Vogels, Brian McWilliams, Mark Meyer, Jan Novák, Alex Harvill, Pradeep Sen, Tony DeRose, and Fabrice Rousselle. 2017. Kernel-Predicting Convolutional Networks for Denoising Monte Carlo Renderings. *ACM Transactions on Graphics (TOG) (Proceedings of SIGGRAPH 2017)* 36, 4 (2017).
- Benedikt Bitterli, Chris Wyman, Matt Pharr, Peter Shirley, Aaron Lefohn, and Wojciech Jarosz. 2020. Spatiotemporal reservoir resampling for real-time ray tracing with dynamic direct lighting. *ACM Transactions on Graphics (TOG)* 39, 4 (2020), 148–1.
- Carsten Dachsbacher, Marc Stamminger, George Drettakis, and Frédo Durand. 2007. Implicit visibility and antiradiance for interactive global illumination. *ACM Transactions on Graphics (TOG)* 26, 3 (2007), 61–es.

- Stavros Diolatzis, Julien Philip, and George Drettakis. 2022. Active Exploration for Neural Global Illumination of Variable Scenes. *ACM Transactions on Graphics* (2022).
- Michaël Gharbi, Tzu-Mao Li, Miika Aittala, Jaakko Lehtinen, and Frédo Durand. 2019. Sample-based Monte Carlo denoising using a kernel-splating network. *ACM Transactions on Graphics (TOG)* 38, 4 (2019), 1–12.
- Jonathan Granskog, Fabrice Rousselle, Marios Papas, and Jan Novák. 2020. Compositional neural scene representations for shading inference. *ACM Transactions on Graphics (TOG)* 39, 4 (2020), 135–1.
- Jon Hasselgren, Jacob Munkberg, Marco Salvi, Anjul Patney, and Aaron Lefohn. 2020. Neural temporal adaptive sampling and denoising. In *Computer Graphics Forum*, Vol. 39. Wiley Online Library, 147–155.
- Mustafa Işık, Krishna Mullia, Matthew Fisher, Jonathan Eisenmann, and Michaël Gharbi. 2021. Interactive Monte Carlo Denoising using Affinity of Neural Features. *ACM Transactions on Graphics (TOG)* 40, 4, Article 37 (2021), 13 pages. <https://doi.org/10.1145/3450626.3459793>
- Csaba Kelemen, László Szirmay-Kalos, György Antal, and Ferenc Csonka. 2002. A simple and robust mutation strategy for the metropolis light transport algorithm. In *Computer Graphics Forum*, Vol. 21. Wiley Online Library, 531–540.
- Alexander Keller, Luca Fascione, Marcos Fajardo, Iliyan Georgiev, Per Christensen, Johannes Hanika, Christian Eisenacher, and Gregory Nichols. 2015. The path tracing revolution in the movie industry. In *ACM SIGGRAPH 2015 Courses*. 1–7.
- Jaroslav Krivánek, Pascal Gautron, Sumanta Pattanaik, and Kadi Bouatouch. 2005. Radiance caching for efficient global illumination computation. *IEEE Transactions on Visualization and Computer Graphics* 11, 5 (2005), 550–561.
- Alexandr Kuznetsov, Nima Khademi Kalantari, and Ravi Ramamoorthi. 2018. Deep Adaptive Sampling for Low Sample Count Rendering. *Computer Graphics Forum* 37 (2018), 35–44.
- Daqi Lin, Markus Kettunen, Benedikt Bitterli, Jacopo Pantaleoni, Cem Yuksel, and Chris Wyman. 2022. Generalized resampled importance sampling: foundations of ReSTIR. *ACM Transactions on Graphics (TOG)* 41, 4 (2022), 1–23.
- Bradford J Loos, Lakulish Antani, Kenny Mitchell, Derek Nowrouzezahrai, Wojciech Jarosz, and Peter-Pike Sloan. 2011. Modular radiance transfer. In *Proceedings of the 2011 SIGGRAPH Asia Conference*. 1–10.
- Bradford J Loos, Derek Nowrouzezahrai, Wojciech Jarosz, and Peter-Pike Sloan. 2012. Delta radiance transfer. In *Proceedings of the ACM SIGGRAPH Symposium on Interactive 3D Graphics and Games*. 191–196.
- Thomas Müller, Fabrice Rousselle, Jan Novák, and Alexander Keller. 2021. Real-time neural radiance caching for path tracing. *ACM Transactions on Graphics (TOG)* 40, 4 (2021), 1–16.
- Oliver Nalbach, Elena Arabadzhyska, Dushyant Mehta, Hans-Peter Seidel, and Tobias Ritschel. 2017. Deep Shading: Convolutional Neural Networks for Screen-Space Shading. *Computer Graphics Forum (Proc. EGSR 2017)* 36, 4 (2017), 65–78.
- Yaobin Ouyang, Shiqiu Liu, Markus Kettunen, Matt Pharr, and Jacopo Pantaleoni. 2021. ReSTIR GI: Path resampling for real-time path tracing. In *Computer Graphics Forum*, Vol. 40. Wiley Online Library, 17–29.
- Peiran Ren, Jiaping Wang, Minmin Gong, Stephen Lin, Xin Tong, and Baining Guo. 2013. Global illumination with radiance regression functions. *ACM Transactions on Graphics (TOG)* 32, 4 (2013), 130.
- Fabrice Rousselle, Wojciech Jarosz, and Jan Novák. 2016. Image-space control variates for rendering. *ACM Transactions on Graphics (TOG)* 35, 6 (2016), 1–12.
- Farnood Salehi, Marco Manzi, Gerhard Roethlin, Romann Weber, Christopher Schroers, and Marios Papas. 2022. Deep Adaptive Sampling and Reconstruction using Analytic Distributions. *ACM Transactions on Graphics (TOG)* 41, 6 (2022), 1–16.
- Dario Seyb, Peter-Pike Sloan, Ari Silvennoinen, Michał Iwanicki, and Wojciech Jarosz. 2020. The design and evolution of the UberBake light baking system. *ACM Transactions on Graphics (Proceedings of SIGGRAPH)* 39, 4 (July 2020). <https://doi.org/10/gg8xc9>
- Ari Silvennoinen and Peter-Pike Sloan. 2021. Moving basis decomposition for precomputed light transport. In *Computer Graphics Forum*, Vol. 40. Wiley Online Library, 127–137.
- Ayush Tewari, Justus Thies, Ben Mildenhall, Pratul Srinivasan, Edgar Treitsch, Wang Yifan, Christoph Lassner, Vincent Sitzmann, Ricardo Martin-Brualla, Stephen Lombardi, et al. 2022. Advances in neural rendering. In *Computer Graphics Forum*, Vol. 41. Wiley Online Library, 703–735.
- Manu Mathew Thomas, Gabor Liktó, Christoph Peters, Sungye Kim, Karthik Vaidyanathan, and Angus G Forbes. 2022. Temporally Stable Real-Time Joint Neural Denoising and Supersampling. *Proceedings of the ACM on Computer Graphics and Interactive Techniques* 5, 3 (2022), 1–22.
- Gregory J Ward, Francis M Rubinstein, and Robert D Clear. 1988. A ray tracing solution for diffuse interreflection. In *Proceedings of the 15th annual conference on Computer graphics and interactive techniques*. 85–92.
- Chuanjun Zheng, Yuchi Huo, Shaohua Mo, Zihua Zhong, Zhizhen Wu, Wei Hua, Rui Wang, and Hujun Bao. 2023. Nelt: Object-oriented neural light transfer. *ACM Transactions on Graphics* 42, 5 (2023), 1–16.
- Kun Zhou, Yaohua Hu, Stephen Lin, Baining Guo, and Heung-Yeung Shum. 2005. Precomputed shadow fields for dynamic scenes. In *ACM SIGGRAPH 2005 Papers*. 1196–1201.
- Matthias Zwicker, Wojciech Jarosz, Jaakko Lehtinen, Bochang Moon, Ravi Ramamoorthi, Fabrice Rousselle, Pradeep Sen, Cyril Soler, and S-E Yoon. 2015. Recent advances in adaptive sampling and reconstruction for Monte Carlo rendering. In *Computer graphics forum*, Vol. 34. Wiley Online Library, 667–681.



Figure 6. Example of our method on different scenes. For each scene, we added a new dynamic object. The original scenes are labeled as static. The 1st column shows path-traced results with 2spp. The next column shows our results with 1spp. It already has 3 to 6 times better quality. The second to last column is our method with adaptive sampling. By redistributing samples to the region of change, we achieve up to 8 times improvement.

Hybrid Rendering for Dynamic Scenes

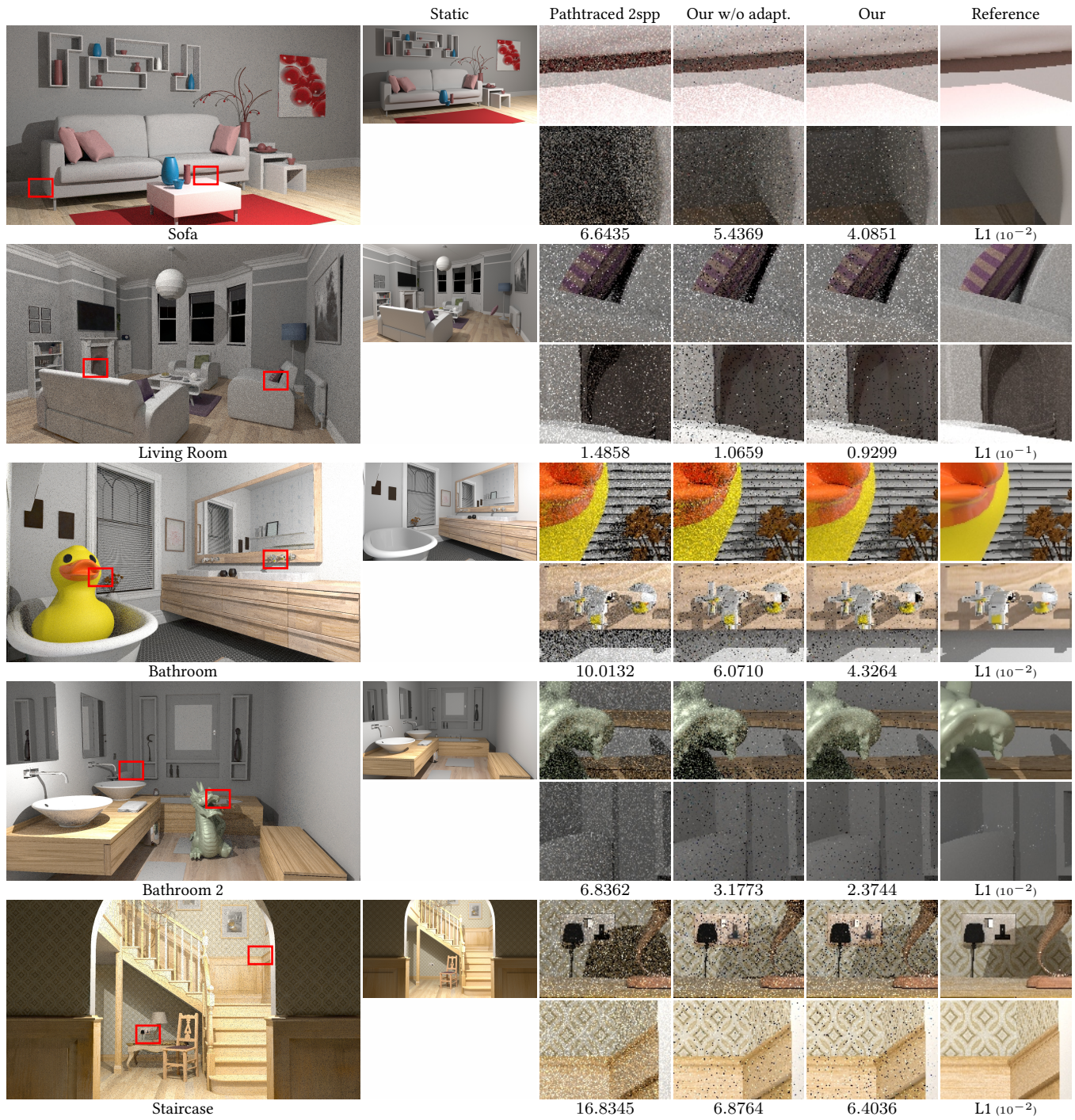


Figure 7. Scenes at different illumination and added objects. When a scene has both kinds of changes, the difference contribution, L_{Δ} becomes more intense and therefore noisier. Despite the amount of changes, our method is still able to outperform the path-tracing.